AIP Journal of Applied Physics

Domain switching energies: Mechanical versus electrical loading in La-doped bismuth ferrite–lead titanate

T. Leist, K. G. Webber, W. Jo, T. Granzow, E. Aulbach, J. Suffner, and J. Rödel

Citation: Journal of Applied Physics **109**, 054109 (2011); doi: 10.1063/1.3555599
View online: http://dx.doi.org/10.1063/1.3555599
View Table of Contents: http://scitation.aip.org/content/aip/journal/jap/109/5?ver=pdfcov
Published by the AIP Publishing

Articles you may be interested in

Effect of tetragonal distortion on ferroelectric domain switching: A case study on La-doped BiFeO 3 – PbTiO 3 ceramics
J. Appl. Phys. **108**, 014103 (2010); 10.1063/1.3445771

Domain switching mechanisms in polycrystalline ferroelectrics with asymmetric hysteretic behavior
J. Appl. Phys. **105**, 024107 (2009); 10.1063/1.3068333

Experimental investigation of domain switching criterion for soft lead zirconate titanate piezoceramics under coaxial proportional electromechanical loading
J. Appl. Phys. **97**, 084105 (2005); 10.1063/1.1870117

High-field dielectric and piezoelectric performance of soft lead zirconate titanate piezoceramics under combined electromechanical loading
J. Appl. Phys. **96**, 6634 (2004); 10.1063/1.1812586

Role of potassium comodification on domain evolution and electrically induced strains in La modified lead zirconate titanate ferroelectric ceramics
J. Appl. Phys. **88**, 3433 (2000); 10.1063/1.1288223

[This article is copyrighted as indicated in the article. Reuse of AIP content is subject to the terms at: http://scitation.aip.org/termsconditions. Downloaded to] IP: 114.70.7.203 On: Tue, 21 Oct 2014 02:29:50

Domain switching energies: Mechanical versus electrical loading in La-doped bismuth ferrite–lead titanate

T. Leist,[1,a)] K. G. Webber,[1] W. Jo,[1] T. Granzow,[1] E. Aulbach,[1] J. Suffner,[1,2] and J. Rödel[1]
[1]*Institute of Materials Science, Technische Universität Darmstadt, 64287 Darmstadt, Germany*
[2]*Institute of Nanotechnology, Karlsruhe Institute of Technology, P.O. 8430, D-76021 Karlsruhe, Germany*

(Received 10 November 2010; accepted 15 January 2011; published online 15 March 2011)

The mechanical stress-induced domain switching and energy dissipation in morphotropic phase boundary $(1-x)(Bi_{1-y}La_y)FeO_3$–$xPbTiO_3$ during uniaxial compressive loading have been investigated at three different temperatures. The strain obtained was found to decrease with increasing lanthanum content, although a sharp increase in strain was observed for compositions doped with 7.5 and 10 at. % La. Increased domain switching was found in compositions with decreased tetragonality. This is discussed in terms of the competing influences of the amount of domain switching and the spontaneous strain on the macroscopic behavior under external fields. Comparison of the mechanically and electrically dissipated energy showed significant differences, discussed in terms of the different microscopic interactions of electric field and stress. © *2011 American Institute of Physics*. [doi:10.1063/1.3555599]

I. INTRODUCTION

Piezoelectric materials are used in many applications such as ultrasonic transducers, actuators in fuel injection nozzles, as well as acceleration and pressure sensors.[1–3] A significant amount of the materials used in these applications are polycrystalline ferroelectrics with perovskite structure, such as PZT. These materials exhibit significant nonlinearity primarily caused by domain wall motion. For maximum achievable displacement in actuator materials non-180° domain motion is especially important. Previous work has shown a maximum in unipolar electric field-induced strain with a preload of approximately −30 MPa, which was discussed as non-180° domain switching generated by preload-induced ferroelastic back-switching.[4,5] The achievable strain is thus closely correlated to the spontaneous strain, e.g., the tetragonal distortion, of the perovskite crystal structure. This implies for certain applications such as high temperature actuators,[1,6,7] where PZT is not ideal due to its relatively low Curie temperature, that a large tetragonality would be beneficial. There are, however, certain limitations. In $PbTiO_3$ ceramics the high tetragonal distortion—quantified by the *c*/*a* ratio—induces high internal stresses within the ceramic when cooling down from the paraelectric cubic phase to the ferroelectric tetragonal phase.[8] For a *c*/*a* ratio of 1.06 these internal stresses are high enough to destroy the ceramic upon cooling from sintering temperatures.[8]

External mechanical compressive stress has been found to strongly influence switching,[9,10] either suppressing or assisting domain reorientation processes.[4,11–22] If the external applied stress is large enough domain switching may be suppressed completely.[12,14] However, small mechanical compressive stresses can also prompt an increase in ferroelectric properties.[4,5,16,19,20] Depending on the orientation of the mechanical load it is possible to improve the domain switching ability of polycrystalline[21,22] and single crystal ferroelectrics.[23] The influence of mechanical load is not limited to external stress; intrinsic internal stress has also been found to influence the switching behavior of ferroelectric materials.[24,25] If the distortion is too large, the internal stress can suppress switching and prevent poling.

$(1-x)(Bi_{1-y}La_y)FeO_3-xPbTiO_3$ (BF-PT) is an ideal model system to investigate the influence of crystallographic distortion on the polarization reversal behavior; substituting lanthanum for bismuth on the A site allows a variation of the *c*/*a* ratio from 1.10 to 1.01.[26,27] A case study on this material showed a near-complete suppression of switching processes due to electrical loading for low La content.[28,29] This effect was attributed to the high internal stresses that are directly related to a large *c*/*a* ratio.[30,31] However, experiments with electric field loading are limited by the breakdown strength and the relatively high conductivity of BF-PT. In order to circumvent these limitations and investigate the potential of non-180° domain switching Kounga Njiwa *et al.*[32] measured the ferroelastic behavior of undoped BF-PT. Their study, however, did not investigate the influence of varying tetragonal distortion on non-180° domain switching.

As a mechanical equivalent to the investigation of electrically induced domain switching,[29] the present paper focuses on the influence of the *c*/*a* ratio on the non-180° domain switching in the model system BF-PT under uniaxial compression at three different temperatures. To date there have been no *in situ* investigations directly showing the affect of external fields on domain wall motion in BF-PT. This work presents indirect experimental evidence of the effect of tetragonality on temperature-dependent ferroelastic behavior. The BF/PT ratio was adjusted to obtain a structure in the region of the morphotropic phase boundary (MPB) for each given La content.[27] From the stress–strain curves the energy dissipated at different maximum loads was assessed[20] and compared to the energy dissipation during electrical

a)Author to whom correspondence should be addressed. Electronic mail: leist@ceramics.tu-darmstdt.de.

 © 2011 American Institute of Physics

[This article is copyrighted as indicated in the article. Reuse of AIP content is subject to the terms at: http://scitation.aip.org/termsconditions. Downloaded to] IP: 114.70.7.203 On: Tue, 21 Oct 2014 02:29:50

poling at various electric field amplitudes.[33] The results elucidate the influence of the tetragonal distortion on non-180° domain switching and energy dissipation of the tetragonal phase in MPB compositions.

II. EXPERIMENTAL PROCEDURES

$(1-x)(Bi_{1-y}La_y)FeO_3-xPbTiO_3$ (BF-PT) solid solutions with eight different lanthanum concentrations, all in the range of the morphotropic phase boundary, were prepared by using a solid oxide route. The material's stoichiometry was chosen so that the fraction of tetragonal and rhombohedral phase in the bulk material is as close to equal as possible. However, it has been shown that even significant deviations from this ratio have little influence on material properties.[27] Details of the powder preparation and sintering procedures can be found in detail elsewhere.[27,29,34] As an effect of the lanthanum doping it was possible to tune the tetragonality from 1.10 to 1.01,[27] which was accompanied by a reduced Curie temperature.[26] The Curie temperature was found to decrease from 632 °C in the undoped material to 189 °C in the material doped with 30 mol. % La.[26,30,35] The materials were investigated in terms of tetragonal distortion because the tetragonal distortion in BF-PT in the MPB region was found to be much higher than the rhombohedral distortion.[29] It is assumed that the tetragonal distortion dominates the level of domain switching and piezoelectric properties of BF-PT.

Cylindrical samples with a diameter of ~5.8 mm and a height of ~6 mm were prepared for uniaxial compression experiments.[34] For electrical and XRD measurements, disks with a thickness of ~0.7 mm were cut from sintered specimens in order to remove the surface layer.[29] To eliminate possible grinding-induced stresses the samples were annealed at 650 °C for 12 min followed by cooling with a rate of 50 °C/h. XRD measurements were carried out on polished and annealed surfaces at various temperatures with a Bruker Siemens D8 station equipped with a hot stage. The diffraction patterns obtained from the XRD measurements were evaluated using the Rietveld refinement software GSAS.[36,37]

A differential dilatometer capable of measuring longitudinal strain at elevated temperature was used to characterize the ferroelastic behavior of BF-PT. This experimental arrangement was previously described in detail.[38,39] Because the electrical boundary conditions were found to have significant effect on the material response during mechanical loading,[40] unpoled samples were mechanically compressed with short-circuit electric boundary conditions in a screw-type load frame (Z010, Zwick, Ulm, Germany) equipped with a thermal chamber. Each unpoled specimen was heated to the target temperature with a rate less than 1.5 °C/min. During heating, a preload of −3.7 MPa was applied to ensure constant contact between the sample and the loading fixture. Each specimen was mechanically loaded/unloaded from this preload at a rate of −3.7 MPa/s to a maximum load of −380 MPa. In a second set of experiments at room temperature, the samples were loaded to progressively larger maximum stress levels with an unloading step to the preload stress between each maximum stress level. For each composition and temperature one cylindrical sample was measured. Due to misalignment and possible compositional differences the errors within these measurements were estimated to be ~5%. The results were quantified in terms of maximum strain ε_{max}, remanent strain ε_r, back-switching strain $(\varepsilon_r^{el}-\varepsilon_r)$, and coercive stress σ_c, which are labeled on a representative ferroelastic curve in Fig. 1. The coercive stress was determined by taking the inflection point of the loading portion of the stress–strain curve, analogous to the poling electric field.[13,17,41,42] The mechanically dissipated energy, G_M, during a mechanical loading cycle can be obtained by integrating the loading and unloading paths to determine the area within the stress–strain curve (Fig. 1).

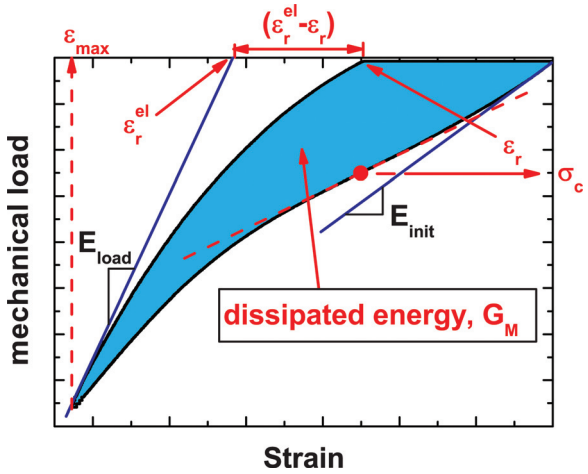

FIG. 1. (Color online) Description of the origin of the remanent strain ε_r, the maximum strain ε_{max}, the back-switching strain $(\varepsilon_r^{el}-\varepsilon_r)$, the dissipated energy G_M and the coercive stress σ_c.

For electrical characterization the disk-shaped samples were electroded with silver paste and measured at room temperature in a Sawyer-Tower circuit. A bipolar triangular voltage signal with a frequency of 4 Hz was applied to the sample. After measuring the poling curve at a certain field the sample was depoled and retested. A Berlincourt meter was used to ensure complete depoling. With this technique poling curves from 1 to 8 kV/mm were measured. Analogous to mechanical loading, the dissipated energy for the electrical loading, G_E, corresponds to the amount of hysteresis under the polarization-electric field curve.

III. RESULTS

The results of the XRD measurements are depicted in Fig. 2, where the *c*/*a* ratios obtained from Rietveld refinement are plotted as a function of the lanthanum concentration for three different temperatures. An increase in the La content leads to a reduction of the *c*/*a* ratio of the tetragonal phase from 1.10 to 1.01, in agreement with previous reports.[26,27] As expected, an increase in temperature leads to a decrease in the tetragonal distortion. Measurement fits are provided to visualize the changes in the *c*/*a* ratios for each temperature. An increase in temperature from room temperature to 100 °C, for example, causes the *c*/*a* ratio to decrease by 10% from approximately 1.10 to approximately 1.09 for the undoped material. Similar results have been reported by Sunder *et al.*[43] and Chen *et al.*[44] It is apparent from Fig. 2 that increasing temperature decreases the tetragonality over

[This article is copyrighted as indicated in the article. Reuse of AIP content is subject to the terms at: http://scitation.aip.org/termsconditions. Downloaded to] IP: 114.70.7.203 On: Tue, 21 Oct 2014 02:29:50

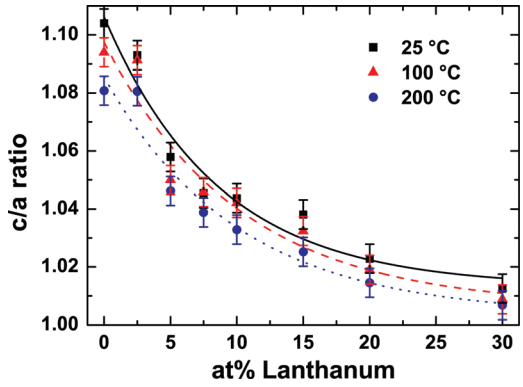

FIG. 2. (Color online) Evolution of the *c*/*a* ratio over the lanthanum doping concentration for different temperatures. The trend for each temperature is visualized using a line with an exponential fit on the measured data. (add another *y* axis showing the corresponding spontaneous strain) make lines a little thicker.

the whole compositional range investigated. However, in comparison to the lanthanum-induced changes in *c*/*a*, the reduction in *c*/*a* that is caused by increasing temperature is comparably small.

Figures 3(a)–3(c) provide representative stress–strain curves of La-doped BF-PT samples with four different lanthanum concentrations (0, 7.5, 15, and 30 at. % La) for the three different temperatures. The shape of the ferroelastic hysteresis curve was found to depend on the lanthanum doping concentration. Samples with low lanthanum content (large tetragonal distortion) and high lanthanum content (small tetragonal distortion) showed limited ferroelastic switching at room temperature. Intermediate compositions, however, those with more moderate critical switching stresses and substantial switching strains, displayed increased hysteresis, maximum and remanent strains, as well as nonlinearity during initial loading.

The coercive stress was determined as the point of inflection in the stress–strain curve during initial loading[13,17,41] and plotted in Fig. 4 as a function of the *c*/*a* ratio. It was not possible to determine a coercive stress for the composition doped with 2.5 at. % lanthanum at room temperature and for the high temperature measurements of the 30 at. % lanthanum-doped sample. For high *c*/*a* (low La doping levels) the coercive stress is around −275 MPa. The coercive stress remained approximately constant until the *c*/*a* ratio was reduced below 1.045 (more than 7.5 at. % lanthanum). Below this *c*/*a* ratio the coercive stress drops sharply by approximately 100 MPa, followed by a more gradual decrease, in analogy to previous work on electric-field-induced switching.[29] This was, however, not observed at 200 °C, where there was an approximately linear decrease in coercive stress with decreasing tetragonality. With increasing temperature the coercive stress was found to decrease further.

For each composition and temperature tested the remanent strain ε_r, maximum strain ε_{max}, and back-switching strain $(\varepsilon_r^{el} - \varepsilon_r)$ were determined from the stress–strain curves. The dissipated energy was also calculated by evaluating the area enclosed by the stress–strain curve. These results are displayed as a function of La content in Figs. 5(a)–5(d). It can be observed for all parameters at room temperature that there is a general trend to decrease with increasing La content, with

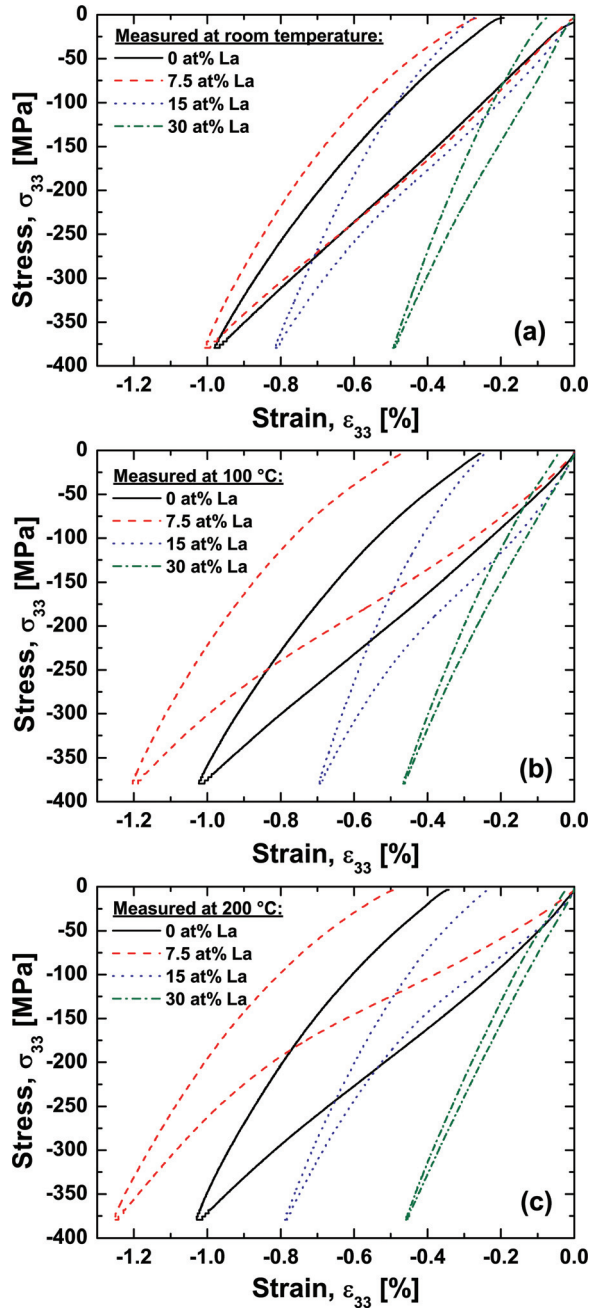

FIG. 3. (Color online) Selected stress–strain curves of 0, 7.5, 15, and 30 at. % La-doped samples measured at (a) room temperature, (b) 100 °C, and (c) 200 °C.

a pronounced discontinuity in the vicinity of 7.5–10 at. % La content. The remanent, maximum, and back-switching strain, as well as mechanically dissipated energy, all showed similar behavior at room temperature. With increasing concentrations of lanthanum an increase in achievable strain was found, corresponding to the observed discontinuous jump in coercive stress (Fig. 4). Remanent strain, back-switching strain, and dissipated energy at doping concentrations below this threshold showed approximately composition-independent behavior, whereas maximum strain, slightly decreased with increasing La content, followed by a broader discontinuity that also included the 10 at. %-doped sample. For all strain measurements, increasing the lanthanum content past 10 at. % resulted in a measured decrease.

[This article is copyrighted as indicated in the article. Reuse of AIP content is subject to the terms at: http://scitation.aip.org/termsconditions. Downloaded to] IP: 114.70.7.203 On: Tue, 21 Oct 2014 02:29:50

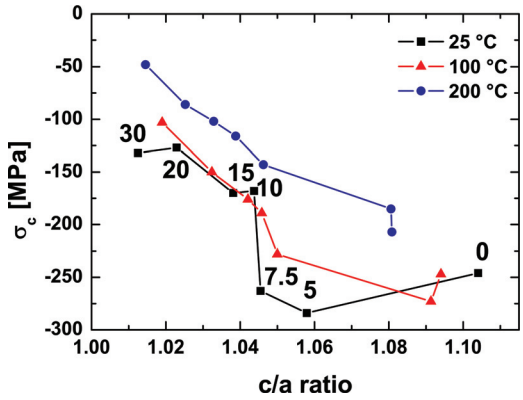

FIG. 4. (Color online) Coercive stress as a function of the *c*/*a* ratio for different temperatures. The numbers on the 25 °C data points represent the respective lanthanum doping concentrations.

Interestingly, the maximum strain of these compositions is found at 7.5 and 10 at. % La [Fig. 5(b)]. This is the case for all investigated temperatures. At room temperature the maximum strain of these two compositions is around −1% for −380 MPa and is increased significantly up to approximately −1.2% for the 7.5 at. % sample with increasing temperature, whereas the observed strain in the undoped sample remains approximately constant. For the 15 and 30 at. % La-doped systems the measured strain is significantly lower than the other compositions, displaying maximum strain values around −0.8 and −0.5%, respectively. Counterintuitively, the maximum strain was found to decrease at 100 °C showing values of approximately −0.7% (15 at. % La) and −0.45% (30 a % La). At 200 °C the strain was again found to increase for the 15 at. % sample, but remained constant for the 30 at. % sample.

It is apparent from Figs. 5(a)–5(d) that an increase in temperature resulted in an increase in ε_r, ε_{max}, back-switching strain, and dissipated energy for compositions doped below approximately 10 at. % La. For each characterizing parameter, however, the opposite was found for compositions above 10 at. % La, i.e., there was a general trend of decreasing material properties with increasing temperature. Notable exceptions to this are maximum and back-switching strain, which are both subject to greater measurement error due to possible misalignment. A transition range between the high- and low-doped systems was found near the observed discontinuity at 7.5–10 at. % La.

In order to assess the effect of the tetragonal distortion on the domain switching behavior, the remanent and back-switching strain were normalized by the spontaneous strain of the unit cell, ε_s, using the following equation[38]:

$$\varepsilon_s = \frac{2(c-a)}{c+2a}. \quad (1)$$

The lattice parameters, *c* and *a*, were taken from the Rietveld refinement of XRD measurements. Interestingly, when the spontaneous strain is considered, both the remanent and back-switching strains show different behaviors than those shown previously in Figs. 5(a) and 5(c). The normalized remanent strain [Fig. 6(a)] shows an initial increase from compositions with the lowest *c*/*a* ratios, followed by two discontinuous "wells" found at approximately 1.02 and 1.04. With a further increase of tetragonality there is a decrease in normalized remanent strain. The back-switching strain, however, still only displays one discontinuity at approximately 1.04, but at high-doping contents it shows a decrease. The exact position of the observed discontinuity was found to depend on temperature, where at 200 °C it was found at lower values of *c*/*a* and 100 °C and room temperature measurements were approximately equivalent. Interestingly, the sample doped with 30 at. % La, with a *c*/*a* ratio of ~1.01, behaves abnormally, insofar as an increase in temperature leads to a decrease in

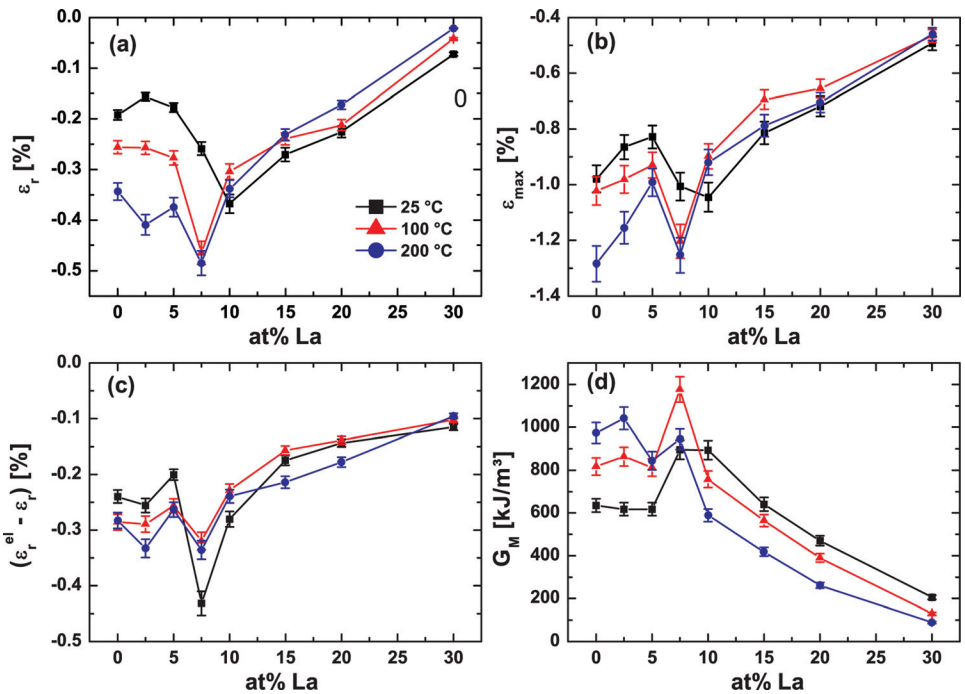

FIG. 5. (Color online) Evolution of (a) the remanent strain ε_r, (b) the maximum strain ε_{max}, (c) the back-switching strain ($\varepsilon_r^{el} - \varepsilon_r$), and (d) the energy dissipated during one load cycle at room temperature, 100 °C, and 200 °C. The small numbers in each plot represent the La doping concentration.

[This article is copyrighted as indicated in the article. Reuse of AIP content is subject to the terms at: http://scitation.aip.org/termsconditions. Downloaded to] IP: 114.70.7.203 On: Tue, 21 Oct 2014 02:29:50

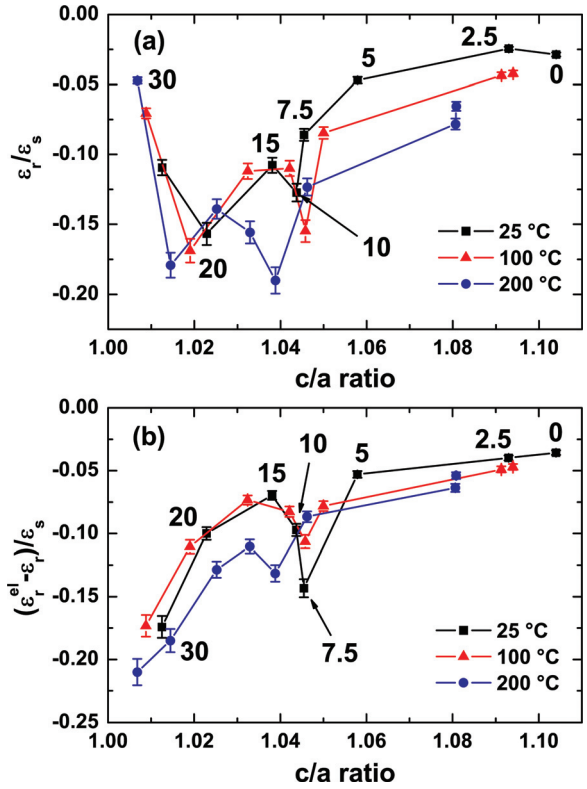

FIG. 6. (Color online) (a) Normalized remanent strain $\varepsilon_r/\varepsilon_s$ and (b) normalized back-switching strain $(\varepsilon^{el}{}_r-\varepsilon_r)/\varepsilon_s$ at room temperature, 100 °C, and 200 °C. The numbers represent the corresponding lanthanum concentration.

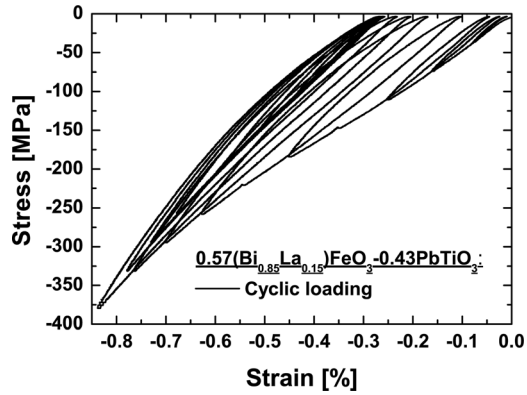

FIG. 7. Representative stress–strain curve obtained during cyclic loading of $0.57(Bi_{0.85}La_{0.15})FeO_3$–$0.43PbTiO_3$.

normalized remanent strain. This same behavior was not found in the normalized back-switching strain.

In order to compare the ferroelectric and ferroelastic switching, cyclic loading and poling measurements have been conducted to evaluate the energy dissipated. Figure 7 illustrates the stress–strain hysteretic behavior during cyclic loading. With increasing maximum compressive stress the overall area under the stress–strain curve (e.g., the dissipated energy during mechanical loading), in addition to the remanent maximum strain, is increased. The analogous electrical case is shown in Fig. 8, where representative poling curves of a low-doped [Fig. 8(a)] and a high-doped [Fig. 8(b)] BF-PT composition are compared. It is apparent in Fig. 8(a) that the polarization has not saturated, despite electrical loading up to 8 kV/mm. The polarization and the area under the curve are gradually increasing for increasing poling fields. The maximum polarization found in this material is around 11 $\mu C/cm^2$, which is relatively low when compared to Fig. 8(b), where the poling curves show clear saturation for poling fields above 6 kV/mm. The increase in polarization and ferroelectric hysteresis (e.g., dissipated electrical energy) were also found to increase with increasing poling fields.

Figure 9 provides the evolution of the dissipated energy for mechanical and electrical loading. As reference, a commercially available soft PZT (PIC 151, PI Ceramics) is also shown for both cases.[45] As expected, an increase in the maximum applied load corresponds to an increase in both mechanically and electrically dissipated energy for all compositions. In agreement with observations made from Figs. 3 and 5(d), it can be observed that the 7.5 and 10 at. % La-doped samples show the highest mechanical energy dissipation. A very pronounced drop in the dissipated energy is observed when the doping content is increased from 15 to 30 at. % La. The energy dissipation behavior of BF-PT was found to be different than that measured for PZT, which exhibits an obvious saturation in dissipated energy. This phenomenon is not visible in BF-PT. For a doping content higher than 10 at. %, however, the possible onset of saturation can be observed, indicating that saturation may occur at increased loading. The electrically induced energy dissipation [Fig. 9(b)] also displays an increase with increasing applied poling fields. It was found that the absolute values of the dissipated energy are significantly higher for most

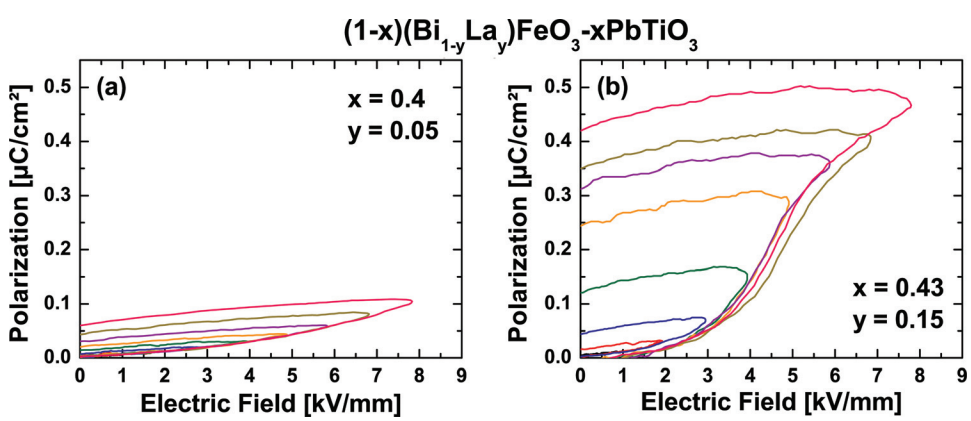

FIG. 8. (Color online) Poling curves for different maximum electric fields exemplarily shown for (a) $0.6(Bi_{0.95}La_{0.05})FeO_3$–$0.4PbTiO_3$ and (b) $0.57(Bi_{0.85}La_{0.15})FeO_3$–$0.43PbTiO_3$.

[This article is copyrighted as indicated in the article. Reuse of AIP content is subject to the terms at: http://scitation.aip.org/termsconditions. Downloaded to] IP: 114.70.7.203 On: Tue, 21 Oct 2014 02:29:50

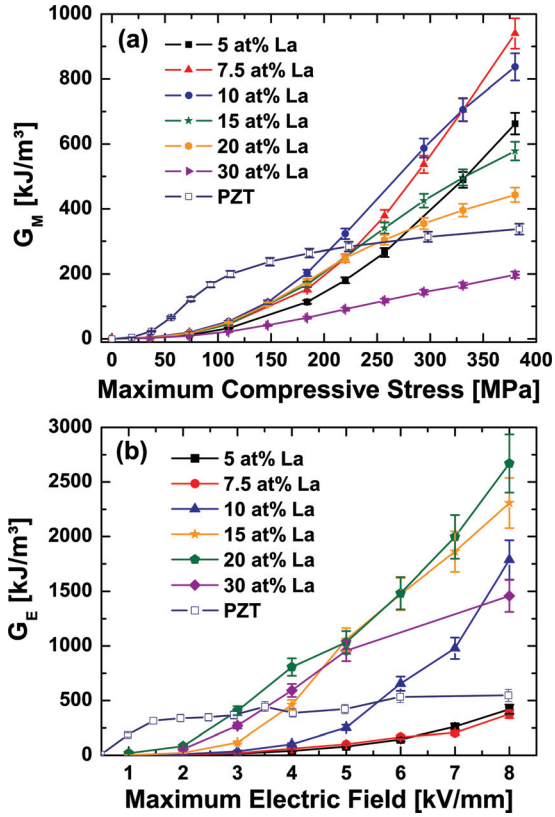

FIG. 9. (Color online) The mechanically dissipated energy as a function of maximum applied load (a), shown for six compositions in comparison to PZT, and the electrically dissipated energy as a function of the poling field shown for six compositions in comparison to PZT (Ref. 45).

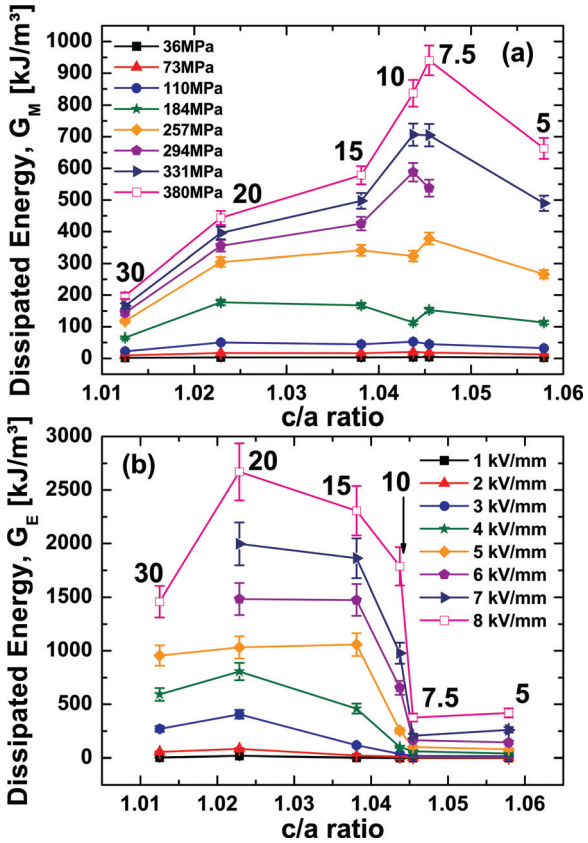

FIG. 10. (Color online) (a) Mechanically dissipated energy and (b) electrically dissipated energy as a function of the *c*/*a* ratio. The numbers represent the corresponding lanthanum doping concentration.

compositions in the electrical case compared to the mechanical case. Interestingly, however, for the systems doped with 5 and 7.5 at. % La, the energy dissipation was comparably low; even up to 8 kV/mm. An increase in the lanthanum content to 10 at. % and more lead to a sharp increase in dissipated energy, with a maximum found for the composition doped with 20 at. % La. Increasing the doping concentration to 30 at. % resulted in a decrease in energy dissipation, with saturation approaching ~8 kV/mm. The energy dissipation of BF-PT is more than five times larger than PZT, although PZT displays a clear saturation point at around 1.5 kV/mm, whereas the possible onset of a saturation point in BF-PT is only visible for 30 at. % La.

Figure 10 shows a direct comparison between the energy dissipated during mechanical, as well as electric, loading and the tetragonal distortion. As each *c*/*a* ratio corresponds to one specific doping concentration, the plot can also be read as dissipated energy as a function of La content. For the mechanical case [Fig. 10(a)] there is not a clear change in the energy dissipation for uniaxial loads from −36 to −110 MPa. The first noticeable changes are found at −184 MPa, where the highest values of the dissipated energy are found to occur at a *c*/*a* ratio of approximately 1.05–1.025 (7.5–20 at. % La). By increasing the load, a peak in energy emerges at a *c*/*a* ratio of ~1.045 (7.5 at. % La) and reaches approximately 940 kJ/m^3 at −380 MPa. Electrically [Fig. 10(b)], almost no dissipated energy can be observed at poling fields of 1 and 2 kV/mm. When the electric field is increased above 2 kV/mm energy dissipation is observed. Samples with *c*/*a* ratios higher than 1.045 dissipate relatively little energy during electrical loading. For compositions with lower *c*/*a* ratios the energy dissipation increases rapidly with maximum electric field, reaching a maximum near 2700 kJ/m^3 at 8 kV/mm for 20 at. % La. For compositions on either side of 20 at. % La there is a significant decrease in energy dissipation. Interestingly, with smaller tetragonal distortions ($c/a < 1045$) the ratio of electrical-to-mechanical dissipated energy at maximum applied stress (−380 MPa) and electric field (8 kV/mm) is found to be between 2 and 5, whereas with larger tetragonal distortions ($c/a > 1.045$) this ratio decreases to approximately 1/2.

IV. DISCUSSION

When applying a mechanical stress or an electric field on a ferroelectric material, strain is generated by linear elastic behavior, the intrinsic piezoelectric effect and non-180° domain switching. The amount of strain that is obtained during loading is affected by the distortion of the corresponding crystal structure and the total number of domain switching. Both are competing factors in La-doped BF-PT: lanthanum doping reduces the tetragonal distortion,[26,27] as does heating to higher temperatures, in agreement with the behavior shown in Fig. 2 and also reported elsewhere.[43,44] This would lead to a decrease in achievable strain from domain switching, however, less tetragonal distortion also means lower internal

[This article is copyrighted as indicated in the article. Reuse of AIP content is subject to the terms at: http://scitation.aip.org/termsconditions. Downloaded to] IP: 114.70.7.203 On: Tue, 21 Oct 2014 02:29:50

stresses, which should, in principle, allow for more domain switching and thus more strain. The results shown in Fig. 3 lead to the following conclusions: first, the changes in strain from 0 to 7.5 at. % La would imply that the increase in the amount of domain switching is more important for compositions up to 7.5 at. % La than the reduction of the *c/a* ratio from 1.10 to 1.045. The temperature-dependent changes for these materials also point to this direction because they display increasing strain with increasing temperature, whereas the temperature-induced reduction in *c/a* ratio is not that pronounced (e.g., from ~1.10 at room temperature to ~1.08 at 200 °C for the undoped sample). Second, at higher La concentrations, the reduction in spontaneous strain becomes the dominating effect. This is also true for the temperature-dependent behavior, which shows a decrease in spontaneous strain (e.g., tetragonal distortion) at increased temperature. From the shape of the stress–strain curves and the absence of a clearly visible coercive stress, it can be concluded that either switching at room temperature takes place over the entire loading range or the nonlinearity is not clearly observed because the strain generated from switching is not significant.

As an effect of the increased temperature, the shape of the stress–strain curves changes; a coercive stress becomes visible and decreases with increasing temperature. Domains that were clamped before are now able to switch, in agreement with Landau theory where an increase in temperature leads to a reduced energy barrier for domain switching,[46] confirmed in Fig. 4 where an increase in temperature decreases the coercive stress. The decrease in the ferroelastic energy barrier is also assisted by the reduction of the *c/a* ratio by ~10% due to the temperature increase. For high *c/a* ratios the changes in σ_c with temperature are more pronounced than the changes at low *c/a* ratios, possibly explaining why for larger tetragonal distortions there is a more drastic change in strain and energy dissipation properties with temperature. It is assumed that the mechanical switching energy barrier in these compositions decreases at a faster rate than the tetragonality, allowing more domains to switch. This was not the case for low *c/a* ratios, where the coercive stress values were not as large. It was assumed that, due to the maximum stress levels used, decreases in coercive stress did not have as significant an impact because even at room temperature most possible ferroelastic switching had already taken place. In addition, the impact of additional ferroelastic switching at elevated temperatures was diminished by smaller spontaneous strains. The room temperature coercive stresses lead to the conclusion that there is a threshold value for domain switching at a *c/a* of 1.045, similar to electrical switching.[29] Coercive stress values for compositions around the threshold *c/a* ratio were found to be in the range of hard-doped PZT,[39] whereas BF-PT materials with high *c/a* ratios are almost twice as high as found for hard-doped PZT. The observed coercive stress of the undoped sample matches the value found by Kounga *et al.*[32] It is, however, not fully understood why this behavior is not apparent in the strain and energy dissipation induced by the mechanical loading experiments. This will be addressed again later in this section.

For lanthanum concentrations of 0–5 at. % the remanent strain, back-switching strain, and dissipated energy remain almost constant, although the tetragonality changes from approximately 1.10 to 1.06. It is assumed, with respect to the two competing aspects discussed in the beginning of this section, that the change in domain switching counterbalances the effect of a reduced spontaneous strain. However, the maximum strain ε_{max} for these compositions shows an increase with increasing lanthanum content (also at elevated temperature). This is because the maximum strain is the product of multiple competing factors, such as the change in Young's modulus as a function of stress,[38,39,47] as well as both the strain generated during domain switching and the amount of domains that are able to switch. For compositions doped with the highest concentrations of lanthanum it was found that the strain response and the dissipated mechanical energy decreased as a function of lanthanum concentration, despite the assumed increase in domain switching. In this range the limiting factor was the relatively small tetragonality. The measured behavior was also found to be less temperature sensitive than with larger *c/a* ratios, most likely due to the smaller coercive stress (Fig. 4) leading to a saturation of domain switching at lower temperatures. Between these two extremes a compositional range was found at 7.5 at. % La, which generally showed maximum strain response and increased hysteretic behavior. This composition combines a high spontaneous strain (tetragonal distortion) with a high amount of domain switching, that in sum results in a maximum strain.

Normalizing the remanent and back-switching strain by the spontaneous strain of the unit cell (Fig. 6) eliminates the contribution of the changing *c/a* ratio, revealing the impact of changes due to increased domain switching and, in the case of back-switching strain, stiffness at maximum applied stress. For the case of remanent strain there was an increase in normalized remanent strain from 30 to 20 at. % La [Fig. 4(a)], which can be attributed to a less stable domain structure accompanied by a higher amount of back-switching at high lanthanum concentrations, as shown in Fig. 6(b). This change in domain stability[29] is most likely connected to changes in the domain structure itself,[48] due to the proximity of the Curie temperature that lies at approximately 189 °C.[26] The proximity of the Curie temperature is most likely the cause of the nonlinear increase in normalized back-switching strain with tetragonality [Fig. 6(b)]. With a further increase of tetragonality there is a general increase in normalized remanent strain, indicating that the amount of non-180° domain switching is decreasing. The discontinuity at 7.5 at. % La, however, is still apparent for both normalized remanent and normalized back-switching strains.

The number of domains that can ferroelastically and ferroelectrically switch increases with the maximum applied mechanical or electrical load (Fig. 9). Saturation is obtained when all available domains have switched, as seen for PZT. It is remarkable that there is almost no sign of saturation to be found for the La-doped BF-PT in either the mechanical or electrical case. This indicates that even at high loads a large amount of domains remain unswitched for both the mechanical [Fig. 9(a)] and electrical loading [Fig. 9(b)], despite of the apparent difference in the behavior of the mechanically and the electrically induced energy dissipation. In Fig. 9(a) the sample doped with 5 at. % La shows lower energy dissipation than the materials doped with 7.5 and 10 at. % La.

[This article is copyrighted as indicated in the article. Reuse of AIP content is subject to the terms at: http://scitation.aip.org/termsconditions. Downloaded to] IP: 114.70.7.203 On: Tue, 21 Oct 2014 02:29:50

Again, there are competing mechanisms due to changing *c/a* ratios: lowering the *c/a* ratio facilitates more domain switching, but results in less energy dissipation per switch. This fact becomes apparent for compositions with more than 10 at. % La as the amount of dissipated energy is continuously reduced. Apparently, the increased number of switching processes does not offset the decrease in dissipated energy for domain switching. Values for the energy dissipation of PZT during electrical loading has been previously presented for a bipolar electric field with a maximum field amplitude of 2 kV/mm, which range between 810 (Ref. 18) and 1382 kJ/m^3 (Ref. 16). However, as it is visible from Fig. 9(b) that a further increase in the maximum field strength does not lead to higher values of energy dissipation.[45]

It is evident from Figs. 9 and 10 that there are important differences between mechanical and electrical loading in the evolution of dissipated energy. Electrical loading, for example, appears to dissipate more energy. Contributions from the conductivity were reduced to negligible levels by using a high measuring frequency (4 Hz). Therefore, a possible explanation for the large difference is electrical depolarizing fields arising during poling by both non-180° and 180° domain switching. As the mechanically induced switching does not create a macroscopic polarization in an unpoled sample and the ordered domain structure associated with it, depolarizing fields are negligible for purely mechanical loading. The overall behavior of the energy dissipated under electrical load is in agreement with the existence of a threshold value of the *c/a* ratio for the electrically induced domain switching,[29] which is not seen in the mechanically induced domain switching. The sample doped with 20 at. % La ($c/a \sim 1.02$) shows the largest amount of dissipated energy regardless of the electric field amplitude; it combines a stable domain structure with a large amount of strain. For higher *c/a* ratios domain clamping becomes more critical, while for lower *c/a* ratios (i.e., for the 30 at. % La-doped sample) the domain structure becomes unstable, resulting in a lower total energy dissipation. The behavior is more complex under mechanical load [Fig. 10(a)]. For mechanical loads from −36 to −184 MPa there is only little domain switching in all BF-PT compositions. Increasing the mechanical load induces additional domain switching up to the maximum load. However, only for the composition doped with 7.5 and 10 at. % there is a high *c/a* ratio (e.g., spontaneous strain) combined with the ability of high domain switching. This results in a peak in dissipated energy that becomes more significant when the amount of domain switching increases. Higher doped compositions dissipate less energy due to the reduction in *c/a* ratio, while the 5 at. %-doped sample shows less energy dissipation due to highly hindered domain switching. The position of the peak is not due to the maximum load that has been chosen. Earlier studies contrasting small- and large-signal behaviors revealed that the influence on the loading amplitude is not critical. This is because the domain switching behavior is primarily influenced by the internal stress level, which is correlated to the *c/a* ratio.[29] Therefore, the observed behavior at around 7.5 at. % lanthanum is due to the optimum composition combining high spontaneous strain with high amount of domain switching.

V. CONCLUSIONS

By comparing the electrical and mechanical response of BF-PT, it has been found that the response to mechanical compressive stress was different than the response to electrical field. Although there is a sharp discontinuity in strain response and energy dissipation at a *c/a* of around 1.045 during electrical loading, a peak in the properties was found during mechanical loading. The ferroelastic measurements demonstrated that changes in the strain and energy dissipation of BF-PT are the results of two competing factors. A reduction in the tetragonal distortion leads to the possibility of increased domain switching, increasing strain and energy dissipation. However, a reduced *c/a* ratio can also reduce the achievable strain and hysteresis for a domain switch due to a reduced spontaneous strain, which also reduces the energy barrier for switching. In BF-PT it has been shown that the impact of these two competing factors changes when reducing the *c/a* ratio below 1.045; a threshold value found in a previous study.[29] For high *c/a* ratios the changes in the amount of domain switching were found to have the highest impact on the material response. Once the *c/a* ratio is reduced below 1.045 the decreasing spontaneous strain becomes critical and material properties are again reduced. The best properties were found for compositions with 7.5 and 10 at. % La, corresponding to a *c/a* of approximately 1.045. Here a large spontaneous strain is combined with a reasonable amount of domain switching. Differences in the energy dissipation between the electrical and mechanical loading were attributed to depolarizing fields due to the ordered domain structure generated during poling.

ACKNOWLEDGMENTS

The authors would like to thank Mie Marsilius for providing the electrical measurements of PZT. This work was supported by the Deutsche Forschungsgemeinschaft under RO-954/20 is a grant number.

[1]R. C. Turner, P. A. Fuierer, R. E. Newnham, and T. R. Shrout, Appl. Acoust. **41**, 299 (1994).
[2]W. Heywang, K. Lubitz, and W. Wersing, *Piezoelectricity* (Springer, Berlin, 2008).
[3]C. A. Randall, A. Kelnberger, G. Y. Yang, R. E. Eitel, and T. R. Shrout, J. Electroceram. **14**, 177 (2005).
[4]I. Kerkamm, P. Hiller, T. Granzow, and J. Rödel, Acta Mater. **57**, 77 (2009).
[5]M. Mitrovic, G. P. Carman, and F. K. Straub, Int. J. Solids Struct. **38**, 4357 (2001).
[6]D. Damjanovic, Curr. Opin. Solid State Mater. Sci. **3**, 469 (1998).
[7]T. R. Shrout, R. E. Eitel, and C. A. Randall, "High performance, high temperature perovskite piezoelectric ceramics," *Piezoelectric Materials in Devices*, Edited by N. Setter (EPFL Swiss Federal Institute of Technology, Lausanne, Switzerland, 2002).
[8]B. Jaffe, W. R. Cook, and H. Jaffe, *Piezoelectric Ceramics* (Academic, New York, 1971).
[9]J. L. Jones, M. Hoffman, and S. C. Vogel, Physica B. **385–386**, 548 (2006).
[10]J. L. Jones, M. Hoffman, and S. C. Vogel, Mech. Mater. **39**, 283 (2007).
[11]H. Cao and A. G. Evans, J. Am. Ceram. Soc. **76**, 890 (1993).
[12]C. S. Lynch, Acta Mater. **44**, 4137 (1996).
[13]A. B. Schäufele and K. H. Härdtl, J. Am. Ceram. Soc. **79** (1996).
[14]D. Fang and C. Li, J. Mater. Sci. **34**, 4001 (1999).
[15]D. Zhou and M. Kamlah, J. Appl. Phys. **96**, 6634 (2004).
[16]D. Zhou, M. Kamlah, and D. Munz, J. Eur. Ceram. Soc. **25**, 425 (2005).
[17]D. Zhou, M. Kamlah, and D. Munz, J. Am. Ceram. Soc. **88**, 867 (2005).
[18]R. Yimnirun, Y. Laosiritaworn, and S. Wongsaenmai, J. Phys. D **39**, 759 (2006).

[This article is copyrighted as indicated in the article. Reuse of AIP content is subject to the terms at: http://scitation.aip.org/termsconditions. Downloaded to] IP: 114.70.7.203 On: Tue, 21 Oct 2014 02:29:50

[19]P. M. Chaplya and G. P. Carman, J. Appl. Phys. **90**, 5278 (2001).
[20]P. M. Chaplya and G. P. Carman, J. Appl. Phys. **92**, 1504 (2002).
[21]F. X. Li, D. N. Fang, and Y. M. Liu, J. Appl. Phys. **100**, 084101 (2006).
[22]T. Granzow, T. Leist, A. B. Kounga, E. Aulbach, and J. Rödel, J. Appl. Phys. **91** (2007).
[23]E. A. McLaughlin, T. Liu, and C. S. Lynch, Acta Mater. **52**, 3849 (2004).
[24]B. S. Kwak, A. Erbil, J. D. Budai, M. F. Chrisholm, L. A. Boatner, and B. J. Wilkens, Phys. Rev. B. **49**, 14865 (1994).
[25]A. Achulhan and C. T. Sun, J. Appl. Phys. **97**, 114103 (2005).
[26]J. R. Cheng and L. E. Cross, J. Appl. Phys. **94**, 5188 (2003).
[27]T. Leist, W. Jo, T. Comyn, A. Bell, and J. Rödel, Jpn. J. Appl. Phys. **48**, 120205 (2009).
[28]T. P. Comyn, T. Stevenson, and A. J. Bell, J. Phys. IV **128**, 13 (2005).
[29]T. Leist, T. Granzow, W. Jo, and J. Rödel, J. Appl. Phys. **108**, 014103 (2010).
[30]S. A. Fedulov, P. B. Ladyzhinskii, I. L. Pyatigorskaya, and Y. N. Venevtsev, Sov. Phys. Solid State **6**, 375 (1964).
[31]A. J. Bell, A. X. Levander, S. L. Turner, and T. P. Comyn, Proc. 16th IEEE ISAF, Nara-city, Japan, (2007), p. 406.
[32]A. B. Kounga Njiwa, E. Aulbach, J. Rödel, S. L. Turner, T. P. Comyn, and A. J. Bell, J. Am. Ceram. Soc. **89**, 1761 (2006).
[33]J. H. Zheng, S. Takahashi, S. Yoshikawa, K. Uchino, and J. W. C. deVries, J. Am. Ceram. Soc. **79**, 3193 (1996).
[34]T. Leist, K. G. Webber, W. Jo, E. Aulbach, J. Rödel, A. D. Prewitt, J. L. Jones, J. Schmidlin, and C. R. Hubbard, Acta Mater. **58**, 5962 (2010).
[35]J. R. Cheng and L. E. Cross, "Lanthanum and gallium co-modified BiFeO3-PbTiO3 crystalline solutions: Lead reduced morphotropic phase boundary (MPB) piezoelectric ceramics", in *IEEE Ultrasonics Symposium* (Honolulu, Hawaii, USA, 2003), p. 354.
[36]A. C. Larson and R. B. Von Dreele, "General Structure Analysis System (GSAS)," Los Alamos National Laboratory Report No. LAUR 86, (2000).
[37]B. H. Toby, J. Appl. Crystallogr. **34** (2001).
[38]K. G. Webber, E. Aulbach, T. Key, M. Marsilius, T. Granzow, and J. Rödel, Acta Mater. **57**, 4614 (2009).
[39]M. Marsilius, K. G. Webber, E. Aulbach, and T. Granzow, J. Am. Ceram. Soc. **93**, 2850 (2010).
[40]F. X. Li and D. N. Fang, Acta. Mater. **53**, 2665 (2005).
[41]H. Grünbichler, J. Kreith, R. Bermejo, P. Supancic, and R. Danzer, J. Eur. Ceram. Soc. **30**, 249 (2010).
[42]A. B. Kounga Njiwa, E. Aulbach, T. Granzow, and J. Rödel, Acta. Mater. **55**, 675 (2007).
[43]V. V. S. S. S. Sunder, A. Halliyal, and A. M. Umarji, J. Mater. Res. **10**, 1301 (1995).
[44]J. Chen, R. Xing, and G. R. Li, Appl. Phys. Lett. **89**, 101914 (2006).
[45]M. Marsilius (Technische Universität Darmstadt, Materials Science, NAW, Darmstadt, 2010).
[46]T. Mitsui, I. Tatsuzaki, and E. Nakamura, *An introduction to the physics of ferroelectrics* (Gordon and Breach Science Publishers, New York, 1976), Vol. 1.
[47]D. Y. Zhou, R. Y. Wang, and M. Kamlah, J. Eur. Ceram. Soc. **30**, 2603 (2010).
[48]Z. A. Li, H. X. Yang, H. F. Tian, J. Q. Li, J. Cheng, and J. Chen, Appl. Phys. Lett. **90**, 182904 (2007).

[This article is copyrighted as indicated in the article. Reuse of AIP content is subject to the terms at: http://scitation.aip.org/termsconditions. Downloaded to] IP: 114.70.7.203 On: Tue, 21 Oct 2014 02:29:50